Recent Changes in Phytoplankton Communities Associated with Rapid Regional Climate Change Along the Western Antarctic Peninsula

Martin Montes-Hugo, *et al.*
Science **323**, 1470 (2009);
DOI: 10.1126/science.1164533

increased in Europe after 1990, in agreement with the AOD changes seen in Figs. 1 and 2. However, many more stations have measured visibility and many have longer histories. The use of emissions to infer aerosols introduces considerable uncertainty in the estimation of aerosol impacts on radiation (*16*).

The ViI AOD over land is a complementary constraint to satellite-derived AOD (*4*, *5*) that is most readily obtained over oceans. The latter includes volcanic and high-level dust contributions that are necessarily excluded by the ViI approach. The AOD estimated from the Advanced Very High Resolution Radiometer (AVHRR) instrument (*17*–*19*) for the period 1991 to 2005, averaged globally over the oceans, indicates a change comparable in magnitude but opposite in sign to that indicated by Fig. 1. Changes seen in regional analyses of these data (*18*, *19*), however, appear to be entirely consistent with those found here, showing decreases in Europe and increases in industrializing Asia. In particular, the strongest decreases (greater than 0.003 $year^{-1}$) indicated in Fig. 2 are over a belt north of the Mediterranean extending into Asia, matching the analyses over the Mediterranean, Black, and Caspian seas (*19*), and the strongest increases (greater than 0.003 $year^{-1}$) are in near-coast industrializing Asia, thereby matching these analyses (*19*). Thus, it would appear that estimates of change over these regions for the period since 1991 might be improved by combining the ViI and AVHRR estimates.

Although increases in the concentrations of many types of aerosols may have contributed to the AOD increase, by far the largest documented changes in aerosols and their precursors are those from the increased use of fossil fuels, in particular SO_2. If so, the changes reported here appear to be inconsistent with the conclusions of the Intergovernmental Panel on Climate Change (IPCC) [(*20*), chapter 2, p. 160], which cited studies concluding that global emissions of sulfate aerosol decreased by 10 to 20 Tg $year^{-1}$ from 1980 to 2000. Those estimates may not have adequately accounted for the 20 Tg $year^{-1}$ increase of sulfate emission over Asia during that period (*21*). Increases in biomass burning of tropical forest and agriculture (*22*, *23*) may also have contributed to increases in AOD. The decrease of AOD in Europe is a consequence of near-constant fossil fuel use coupled with a large decrease in sulfur content as required by air quality regulations.

Current descriptions of AOD as provided by satellite data (*6*) have been used as a major constraint on the aerosol radiative forcing used as part of the IPCC modeling of climate change (*4*, *5*). However, the objective of simulating the 20th-century climate as a means of validating the models has been limited by an absence of observational information on the time history of AOD, a shortcoming that is remedied by the data set described here.

References and Notes

1. M. Wild *et al.*, *Science* **308**, 847 (2005).
2. D. I. Stern, *Glob. Environ. Change* **16**, 207 (2006).
3. J. R. Norris, M. Wild, *J. Geophys. Res.* **112**, D08214 (2007).
4. N. Bellouin, O. Boucher, J. Haywood, M. S. Reddy, *Nature* **438**, 1138 (2005).
5. H. Yu *et al.*, *Atmos. Chem. Phys.* **6**, 613 (2006).
6. See supporting material on *Science* Online.
7. T. W. Biggs, C. A. Scott, B. Rajagopalan, H. N. Turral, *Int. J. Climatol.* **27**, 1505 (2007).
8. Y. Qian, D. P. Kaiser, L. R. Leung, M. Xu, *Geophys. Res. Lett.* **33**, L01812 (2006).
9. H. C. Power, *Theor. Appl. Climatol.* **76**, 47 (2003).
10. J. R. Norris, M. Wild, *J. Geophys. Res.* **112**, D08214 (2007).
11. C. Ruckstuhl *et al.*, *Geophys. Res. Lett.* **35**, L12708 (2008).
12. V. Vestreng, M. Adams, J. Goodwin, *Inventory Review 2004: Emission Data Reported to CLRTAP and the NEC Directive. EMEP/EEA Joint Review Report* (Norwegian Meteorological Institute, Oslo, 2004).
13. D. G. Streets *et al.*, *J. Geophys. Res.* **108**, 8809 (2003).
14. A. Ito, J. E. Penner, *Global Biogeochem. Cycles* **19**, GB2028 (2005).
15. T. Novakov *et al.*, *Geophys. Res. Lett.* **30**, 1324 (2003).
16. J. M. Haywood, O. Boucher, *Rev. Geophys.* **38**, 513 (2000).
17. M. I. Mishchenko *et al.*, *Science* **315**, 1543 (2007).
18. M. I. Mishchenko, I. V. Geogdzhayev, *Opt. Express* **15**, 7423 (2007).
19. T. X.-P. Zhao *et al.*, *J. Geophys. Res.* **113**, D07201 (2008).
20. Intergovernmental Panel on Climate Change, *Climate Change 2007: The Physical Science Basis. Contribution of Working Group I to the Fourth Assessment Report of the Intergovernmental Panel on Climate Change*, S. Solomon *et al.*, Eds. (Cambridge Univ. Press, Cambridge, 2007).
21. T. Ohara *et al.*, *Atmos. Chem. Phys.* **7**, 4419 (2007).
22. C. Venkataraman, G. Habib, A. Eiguren-Fernandez, A. H. Miguel, S. K. Friedlander, *Science* **307**, 1454 (2005).
23. A. L. Westerling, H. G. Hidalgo, D. R. Cayan, T. W. Swetnam, *Science* **313**, 940 (2006); published online 5 July 2006 (10.1126/science.1128834).
24. We thank A. Riter for her editing and proofreading of the manuscript. GSOD data are available at ftp://ftp.ncdc.noaa.gov/pub/data/gsod.

Supporting Online Material

www.sciencemag.org/cgi/content/full/323/5920/1468/DC1
Materials and Methods
Figs. S1 to S7
Table S1
References

22 October 2008; accepted 23 January 2009
10.1126/science.1167549

Recent Changes in Phytoplankton Communities Associated with Rapid Regional Climate Change Along the Western Antarctic Peninsula

Martin Montes-Hugo,[1] Scott C. Doney,[2] Hugh W. Ducklow,[3] William Fraser,[4] Douglas Martinson,[5] Sharon E. Stammerjohn,[6] Oscar Schofield[1]

The climate of the western shelf of the Antarctic Peninsula (WAP) is undergoing a transition from a cold-dry polar-type climate to a warm-humid sub-Antarctic–type climate. Using three decades of satellite and field data, we document that ocean biological productivity, inferred from chlorophyll a concentration (Chl a), has significantly changed along the WAP shelf. Summertime surface Chl a (summer integrated Chl a ~63% of annually integrated Chl a) declined by 12% along the WAP over the past 30 years, with the largest decreases equatorward of 63°S and with substantial increases in Chl a occurring farther south. The latitudinal variation in Chl a trends reflects shifting patterns of ice cover, cloud formation, and windiness affecting water-column mixing. Regional changes in phytoplankton coincide with observed changes in krill (*Euphausia superba*) and penguin populations.

Over the past several decades, the marine ecosystem along the western continental shelf of the Antarctic Peninsula (WAP) (62° to 69°S, 59° to 78°W, ~1000 by 200 km) has undergone rapid physical climate change (*1*). Compared with conditions in 1979 at the beginning of satellite data coverage, seasonal sea ice during 2004 arrived 54 ± 9 (1 SE) days later in autumn and departed 31 ± 10 days earlier in spring (*2*). Winter air temperatures, measured between 62.2°S, 57.0°W and 65.3°S, 64.3°W, warmed at up to 4.8 times the global average rate during the past half-century (*3*–*5*). This warming is the most rapid of the past 500 years and stands in contrast to a marked cooling between 2700 and 100 years before the present (*5*–*7*). As the once-perennial sea ice and glaciers retreat (*6*, *8*), maritime conditions are expanding southward to displace the continental, polar system of the southern WAP (*9*).

As a result, populations of sea ice–dependent species of lower and higher trophic levels are being demographically displaced poleward and are being replaced by ice-avoiding species (e.g.,

[1]Coastal Ocean Observation Lab, Institute of Marine and Coastal Sciences, School of Environmental and Biological Sciences, Rutgers University, New Brunswick, NJ 08901, USA. [2]Department of Marine Chemistry and Geochemistry, Woods Hole Oceanographic Institution, Woods Hole, MA 02543, USA. [3]The Ecosystems Center, Marine Biological Laboratory, Woods Hole, MA 02543, USA. [4]Polar Oceans Research Group, Post Office Box 368, Sheridan, MT 59749, USA. [5]Lamont-Doherty Earth Institute, Palisades, NY 10964, USA. [6]Ocean Sciences, University of California, Santa Cruz, CA 95064, USA.

*To whom correspondence should be addressed. E-mail: montes@marine.rutgers.edu

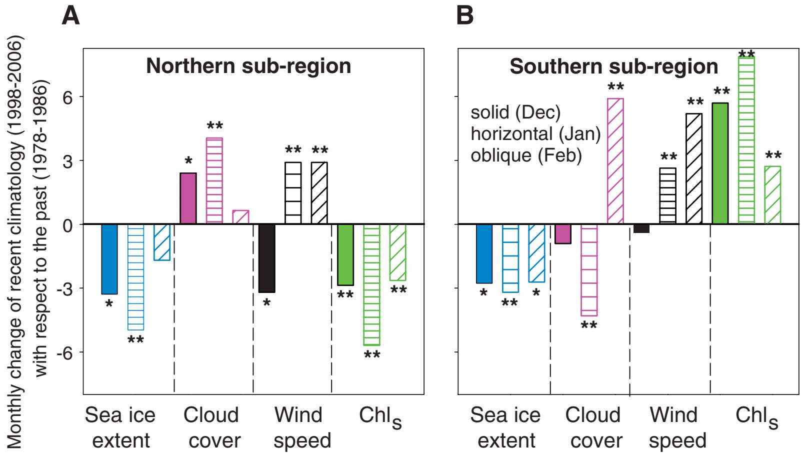

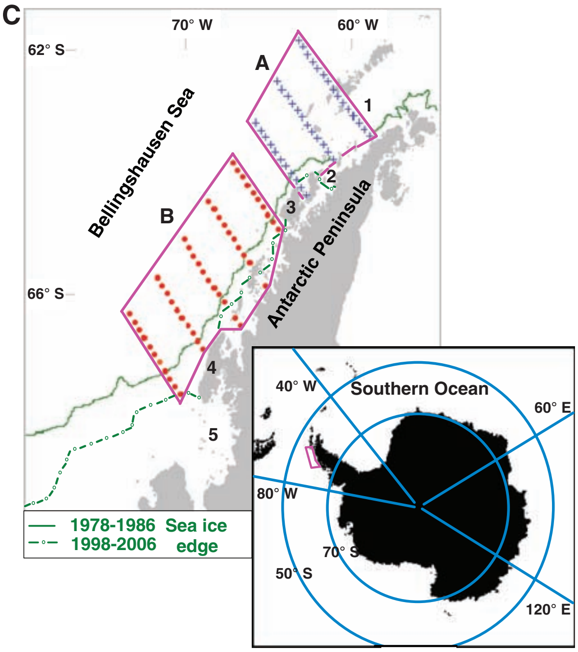

Fig. 1. Decadal variation of phytoplankton biomass and environmental factors along the WAP in (**A**) the northern WAP subregion and (**B**) the southern WAP subregion. Chl$_S$ is chlorophyll a concentration data derived from satellites (1978 to 1986 and 1998 to 2006). Decadal variations (present – past) of mean Chl$_S$ during December (solid bar), January (horizontal stripes), and February (oblique stripes) were evaluated for 1998 to 2006 with respect to the 1978 to 1986 baseline using a Student *t* test. For each variable (*x* axis), the absolute value of the *t* test statistic was multiplied by the sign of the trend (–1, decrease; +1, increase) of the present monthly mean with respect to the mean of the historical period (*y* axis). For January and February, Student *t* of Chl$_S$ was divided by 5. Significant differences between the periods at 95% (*) and 99% (**) confidence levels are indicated. (**C**) Spatial domains A (northern subregion) and B (southern subregion) overlap the original transects of the Palmer-LTER regional grid, where ship-based stations are denoted by blue crosses and red circles, respectively. 1, Bransfield Strait; 2, Gerlache Strait; 3, Anvers Island; 4, Adelaide Island; 5, Marguerite Bay. Average January sea ice extent during 1978 to 1986 (solid green line) and 1998 to 2006 (broken dotted green line) is indicated.

krill are being replaced by salps, and Adélie penguins by Chinstrap penguins) (*1*, *10*, *11*). Do these biogeographic modifications originate from changes at the base of the food web?

In the short term (monthly-interannual scale) and during spring and summer, variations in latitudinal gradients in phytoplankton biomass as a function of time have been associated with sea ice timing and extent (*12*, *13*). However, this mechanism has not been investigated over a longer time scale of decades. Further, the relative importance of subregional differences in climate variables other than sea ice (e.g., cloudiness and currents) in determining WAP alongshore phytoplankton dynamics is not known. In contrast to previous work, we suggest that alongshore phytoplankton distribution in this region has been adjusting to the ongoing, long-term sea ice decline and spatial modifications of other physical climate factors. Short-term evidence from seasonal cruises (*13*–*15*) suggests an inverse relationship between phytoplankton biomass in surface waters (0- to 50-m depth) and the depth of the upper mixed layer (UML). As the UML becomes less stratified, mean light levels for phytoplankton photosynthesis decrease, and phytoplankton growth is not large enough compared with Chl a loss (e.g., grazing and sinking) to support Chl a accumulation in surface waters (*14*). Because deepening of UML is mainly determined by greater surface wind stress (*14*), particularly during ice-free conditions, the expectation is for a general decrease (increase) of phytoplankton biomass at <64°S (>64°S) due to deeper (shallower) UML given a shorter (longer) sea ice season and greater (smaller) influence of wind in determining UML depth and, therefore, mean light levels.

Table 1. Field validation satellite-based chlorophyll a concentration changes between the summers of 1978 to 1986 (past period) and 1998 to 2006 (present period), calculated for the northern and southern WAP subregions. Chl_s^{past} is the monthly average of satellite-derived Chl a (mg m^{-3}) from 1978 to 1986; $dChl_s^{(present-past)}$ is the arithmetic average of pixel-by-pixel differences in satellite-derived Chl a between the 1978 to 1986 period and the 1998 to 2006 period; $dChl_s$% and $dChl_{in\ situ}$% are relative changes in monthly averaged Chl a [100 (Chl $a_{1998\text{-}2006}$ – Chl $a_{1978\text{-}1986}$)/Chl $a_{1978\text{-}1986}$] based on satellite-derived and shipboard Chl a measurements, respectively. Significant increase (+) or decrease (–) of Chl a indicated with a confidence limit of 95% (*) and 99% (**); two SE shown in parentheses.

Subregion		Chl_s^{past}	$dChl_s^{(present-past)}$	$dChl_s$%	$dChl_{in\ situ}$%
Northern	December	1.39 (0.11)	–1.36 (0.26)**	–97.8**	
	January	5.59 (0.20)	–5.43 (0.26)**	–97.1**	–25.2*
	February	2.96 (0.18)	–2.12 (0.49)**	–71.6**	–74.0**
Southern	December	0.89 (0.03)	+1.25 (0.08)**	+140.4**	
	January	0.89 (0.02)	+0.49 (0.03)**	+55.1**	+228.6**
	February	0.94 (0.03)	+0.02 (0.14)	+2.1	–13.6

Based on Chl a concentration derived from satellites [Coastal Zone Color Scanner (CZCS) and Sea-Viewing Wide Field-of-View Sensor (SeaWiFS)] (Chl$_S$) and in situ shipboard measurements (Chl$_{in\ situ}$) (*16*), we report a two-decadal (1978–1986 to 1998–2006) increase (decrease) of biomass in summer (December to February) phytoplankton populations in the continental shelf waters situated south (north) with respect to the central part of the WAP region (Palmer Archipelago, 64.6°S, 63.6°W). These spatial trends were mainly associated with geographic differences in receding sea ice cover and solar illumination of the sea surface.

Since the 1970s, there has been a 7.5% areal decline in summer sea ice throughout the WAP, with the declines varying regionally (Fig. 1, blue bars, and fig. S5, A and E). Cloudiness (Fig. 1, pink bars, and fig. S5, B and F) and wind patterns (Fig. 1, black bars, and fig. S5, C and G) have also changed during the past decade. In the 1970s, overcast skies tended to be positively associated with windy conditions, but in the past 10 years this covariation has weakened considerably (fig. S5, B, C, F, and G). Surface winds have become more intense (up to 60% increase) during mid to late summer (January and February) (Fig. 1 and fig. S5, C to G). Overall, these climate variations were associated with a 12% decline in Chl$_S$ over the entire study region (Table 1) that resembles Chl$_S$ declines reported in northern high latitudes (>40°N) between 1979–1986 and 1997–2000 (*17*).

In the northern subregion of the WAP (61.8° to 64.5°S, 59.0° to 65.8°W), the skies have become cloudier, winds persistently stronger (monthly mean up to 8 m s^{-1}), and summer sea ice extent less, conditions favoring deeper wind-mixing during the months most critical for phytoplankton growth (December and January) (Fig. 1 and fig. S5, A to D). Hence, phytoplankton cells inhabiting these waters have been exposed to a deeper mixed layer and overall less light for photosynthesis (*14*) that may explain the dramatic Chl_S decrease (seasonal average, 89%) detected in recent years (Fig. 1, Fig. 2A, and fig. S5D). Additionally, recent declines of Chl a over the northern WAP subregion might also be partially related to a greater advection of relatively poor–Chl a waters coming from the Weddell Sea into the Bellingshausen Sea through the Bransfield and Gerlache Straits (*18*). A Chl a decrease was less evident during February (Table 1), which suggests that increased mixing early in the growth season caused a lag in phytoplankton bloom initiation but did not influence Chl a levels as strongly later in the growth season. Two possible trigger mechanisms for such a delay are stronger winds [up to 5.4% increase, January (table S5)] and an insufficient volume of fresh water from melting sea ice [up to 79% less sea ice, December (table S5)] that otherwise would create a favorable, strongly stratified, shallow UML (*13*–*15*).

In the southern subregion of the WAP (63.8° to 67.8°S, 64.4° to 73.0°W), remotely sensed Chl a has undergone a remarkable increase (66% on average) from 1978–1986 to 1998–2006 (Fig. 1, fig. S5H, Fig. 2A, and Table 1) that can be attributed mainly to high Chl_S values (monthly mean up to 6.58 mg m^{-3}) during 2005 and 2006. These years were characterized by a substantial decrease in sea ice extent (~17.4 × 10^3 km^2, ~80% with respect to the 1978 to 1986 average, December), cloud cover (~11.1%, January), and wind intensity (up to 19%, December and January) (Fig. 1, fig. S5, E to G, and table S5). Unlike the northern WAP, the decrease in summer sea ice extent in the southern WAP has occurred in areas that were previously sea ice covered most of the year. Therefore, the increase in ice-free summer days translates into more favorable conditions in the UML (e.g., increased light) for phytoplankton growth. Together these environmental changes are expected to enhance photosynthesis and favor Chl a accumulation due to lower light limitation.

Regions with high Chl a levels in the WAP are characterized by a larger fraction of phytoplankton with fucoxanthin, a pigment marker for diatoms, and a larger fraction of relatively large cells (>20 μm) (contribution of cells >20 μm to total Chl a ≥ 0.5) (Fig. 2B). Therefore, the observed trends of decreasing Chl a in the northern subregion and increasing Chl a in the southern subregion are likely accompanied by shifts in community composition with a greater (lesser) fraction of diatoms and large cells in the southern (northern) region. This restructuring of the phytoplankton community has major implications for biogeochemical cycles of the WAP region. Large (>5 μm) phytoplankton contribute 80% of the particulate organic carbon export at high latitudes, with diatoms making up the majority of large phytoplankton export in the Southern Ocean (*19*).

Historical shipboard measurements of Chl a within the study area confirmed the general north-south transitions seen in the satellite data with higher (lower) phytoplankton biomass in the southern (northern) WAP subregion in the past decade compared with 1978 to 1986 (Table 1 and tables S3 and S4). In fact, available field measurements during January and February evidenced a greater occurrence of phytoplankton blooms (Chl a > 5 mg m^{-3}) in the northern (southern) WAP subregion from 1978 to 1986 (1987 to 2006) (SOM Text, S6D) (*16*).

In the northern WAP, the maximum chlorophyll values measured by satellite (up to 40 mg m^{-3}, January) or in situ (up to 38 mg m^{-3}, February) were larger in the past (1978 to 1986) compared with the present (1997 to 2006). Conversely, in the southern WAP this pattern was reversed, and spaceborne and shipborne observations consistently showed higher pigment values in the last decade (satellite, up to 33 mg m^{-3}; ship, up to 25 mg m^{-3}, January) (tables S4 and S5). Monthly Chl a differences between northern and southern WAP locations were also statistically coherent

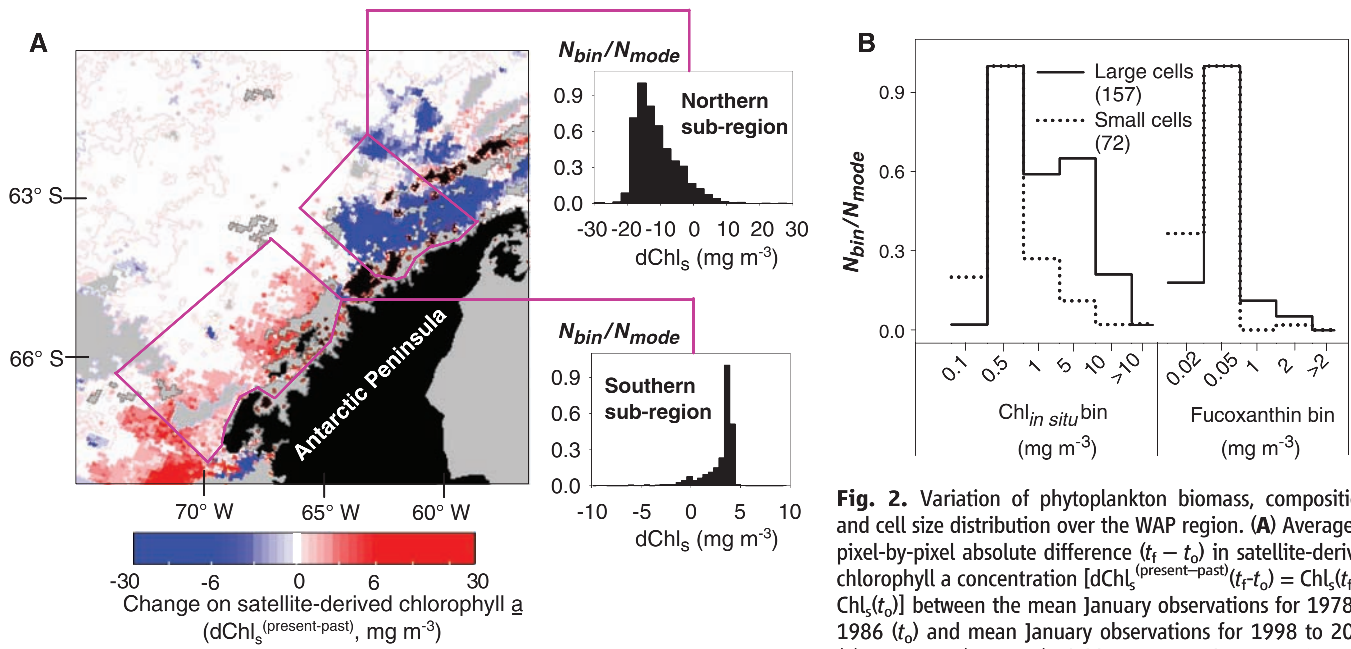

Fig. 2. Variation of phytoplankton biomass, composition, and cell size distribution over the WAP region. (**A**) Average of pixel-by-pixel absolute difference ($t_f - t_o$) in satellite-derived chlorophyll a concentration [$dChl_s^{(present-past)}(t_f$-$t_o) = Chl_s(t_f) - Chl_s(t_o)$] between the mean January observations for 1978 to 1986 (t_o) and mean January observations for 1998 to 2006 (t_f). Positive (negative) $dChl_s$ corresponds to an increase (decrease) of Chl_s with respect to the 1970s. Negative (by a factor of ~2, northern subregion, upper histogram) and positive (by a factor of ~1.5, southern subregion, lower histogram) trends in Chl_s are evident in the satellite data. N_{bin}/N_{mode} is the relative frequency of observations per bin, normalized by the mode. Gray pixels indicate areas without data or without valid geophysical retrieval due to cloud and sea ice contamination; black pixels indicate land. (**B**) Histograms of contribution of diatoms (fucoxanthin marker) and phytoplankton communities dominated by large (≥20 μm) versus small (<20 μm) cell diameter to total in situ chlorophyll a concentration ($Chl_{in\ situ}$). Phytoplankton cell size spectra were computed from satellite imagery (1998 to 2006) (*16*), and phytoplankton pigments were measured over the northern and southern WAP subregions and during 1993 to 2006 Palmer-LTER cruises. Number of samples used to construct each histogram shown in parentheses.

with satellite-derived and field Chl a trends, and in both cases latitudinal phytoplankton biomass gradients were greater during January compared with February (Fig. 1 and tables S4 and S5).

Our study provides evidence for the occurrence of substantial and statistically significant latitudinal shifts at the base of the Antarctic Peninsula marine food web that may be contributing to observations of an apparent reorganization of northern WAP biota during the past decade [e.g., *Euphausia superba* (Antarctic krill), *Pleuragramma antarcticum* (Antarctic silverfish), and *Pygoscelis Adeliae* (Adélie penguin)] that rely on ice-edge diatom blooms (20, *21*). The southward relocation of phytoplankton patches with abundant and large cells (>20 μm) due to local alterations in environmental variables is expected to exacerbate the reduction of krill abundance in the northern WAP. This represents a setback for the survival of fish (silverfish) and birds (Adélie penguins) that depend on krill but favors other species, including *Electrona antarctica* (Lanternfish), *Pygoscelis papua* (Gentoo penguin), and *Pygoscelis antarcticus* (Chinstrap penguin) (*21*, *22*).

The observed latitudinal response of phytoplankton communities along the WAP with respect to historical sea ice variability can be compared with that estimated from geological proxies for similar paleo-oscillations in sea ice extent and rate of change identified during the Holocene (*5*, *23*, *24*). Paleo-records show that analogous climate variations have occurred in the past 200 to 300 years, and over longer 2500-year cycles, with rapid (decadal) transitions between warm and cool phases in the WAP (*5*, *25*, *26*). In this study (~30 years), the Chl a trend evidenced in the southern subregion of the WAP presented similar characteristics to those trends detected during typical interneoglacial periods (~200 to 300 years) (i.e., high phytoplankton biomass, and presumably productivity, due to less area covered by permanent sea ice) (*26*). Since the 1970s, Chl a trends over the whole WAP were also attributed to other factors not necessarily ice-related (e.g., spatial differences in cloud cover) (*27*) or coupled with the length of the ice-free season (e.g., wind-driven changes in mixed layer depth) (*14*, *15*, *28*) that were equally important in determining phytoplankton blooms.

This work suggests that a combination of atmosphere-, ice-, and ocean-mediated processes have been shaping the along-shelf distribution of phytoplankton biomass over the WAP region since the 1970s. The shift toward higher Chl a to the south was first detected using ocean color imagery and subsequently confirmed with in situ historical measurements. The spatial asymmetry of decadal changes in Chl a reported here may explain the ongoing latitudinal compositional changes in fish, zooplankton, and marine bird species over the WAP, a testimonial to which may be the recent success of krill recruitment and the bonanza of krill feeders in nearby Marguerite Bay (68.3°S, 68.3°W) (*29*).

References and Notes

1. H. W. Ducklow *et al.*, *Philos. Trans. R. Soc. London Ser. B* **362**, 67 (2007).
2. S. E. Stammerjohn *et al.*, *Deep Sea Res. Part II Top. Stud. Oceanogr.* **55**, 2041 (2008).
3. D. G. Vaughan *et al.*, *Clim. Change* **60**, 243 (2003).
4. L. G. Thompson *et al.*, *Ann. Glaciol.* **20**, 420 (1994).
5. A. Leventer *et al.*, *Geol. Soc. Am. Bull.* **108**, 1626 (1996).
6. J. Turner *et al.*, *Int. J. Climatol.* **25**, 279 (2005).
7. H. D. Pritchard, D. G. Vaughan, *J. Geophys. Res.* **112**, F03S29 (2007).
8. A. J. Cook *et al.*, *Science* **308**, 541 (2005).
9. R. C. Smith, S. E. Stammerjohn, *Ann. Glaciol.* **33**, 493 (2001).
10. R. C. Smith *et al.*, *Bioscience* **49**, 393 (1999).
11. V. Loeb *et al.*, *Nature* **387**, 897 (1997).
12. R. Smith *et al.*, *Deep Sea Res. Part II Top. Stud. Oceanogr.* **55**, 1949 (2008).
13. I. A. Garibotti *et al.*, *Mar. Ecol. Prog. Ser.* **261**, 21 (2003).
14. G. Mitchell, O. Holm-Hansen, *Deep-Sea Res.* **38**, 981 (1991).
15. M. Vernet *et al.*, *Deep Sea Res. Part II Top. Stud. Oceanogr.* **55**, 2068 (2008).
16. Materials and methods are available as supporting material on *Science* Online.
17. W. W. Gregg, M. E. Conkright, *Geophys. Res. Lett.* **29**, 1730 (2002).
18. M. A. Bárcena *et al.*, *Deep Sea Res. Part II Top. Stud. Oceanogr.* **49**, 935 (2002).
19. X. Jin *et al.*, *Global Biogeochem. Cycles* **20**, GB2015 (2006).
20. M. A. Moline *et al.*, *Ann. N. Y. Acad. Sci.* **1134**, 267 (2008).
21. G. A. Knox, *Biology of the Southern Ocean* (CRC Press, Boca Raton, FL, ed. 2, 2006).
22. W. Fraser, E. E. Hoffmann, *Mar. Ecol. Prog. Ser.* **265**, 1 (2003).
23. M. J. Bentley *et al.*, *Geology* **33**, 173 (2005).
24. C. J. Pudsey, J. Evans, *Geology* **29**, 787 (2001).
25. E. W. Domack, C. E. McClennen, in R. Ross, E. Hofmann, L. Quetin, Eds., *Foundations for Ecosystem Research West of the Antarctic Peninsula* (Antarctic Research Series, Vol. 70) (American Geophysical Union, Washington, DC, 1996).
26. J. Fabrés *et al.*, *Holocene* **10**, 703 (2000).
27. P. R. Burkholder, E. F. Mandelli, *Limnol. Oceanogr.* **57**, 437 (1965).
28. R. B. Dunbar *et al.*, *J. Geophys. Res.* **103**, 30741 (1998).
29. M. Marrari *et al.*, *Deep-Sea Res.* **55**, 377 (2008).

30. This research is part of the Palmer Antarctica Long-Term Ecological Research (LTER) project (http://pal.lternet.edu). It was supported by NSF Office of Polar Programs grants 0217282 to H.W.D. and the Virginia Institute of Marine Science and 0823101 to H.W.D. at the Marine Biological Laboratory.

Supporting Online Material
www.sciencemag.org/cgi/content/full/323/5920/1470/DC1
Materials and Methods
SOM Text
Figs. S1 to S5
Tables S1 to S9
References

11 August 2008; accepted 12 January 2009
10.1126/science.1164533

A Recessive Mutation in the APP Gene with Dominant-Negative Effect on Amyloidogenesis

Giuseppe Di Fede,[1] Marcella Catania,[1] Michela Morbin,[1] Giacomina Rossi,[1] Silvia Suardi,[1] Giulia Mazzoleni,[1] Marco Merlin,[1] Anna Rita Giovagnoli,[1] Sara Prioni,[1] Alessandra Erbetta,[2] Chiara Falcone,[3] Marco Gobbi,[4] Laura Colombo,[4] Antonio Bastone,[4] Marten Beeg,[4] Claudia Manzoni,[4] Bruna Francescucci,[5] Alberto Spagnoli,[5] Laura Cantù,[6] Elena Del Favero,[6] Efrat Levy,[7] Mario Salmona,[4] Fabrizio Tagliavini[1]*

β-Amyloid precursor protein (APP) mutations cause familial Alzheimer's disease with nearly complete penetrance. We found an APP mutation [alanine-673→valine-673 (A673V)] that causes disease only in the homozygous state, whereas heterozygous carriers were unaffected, consistent with a recessive Mendelian trait of inheritance. The A673V mutation affected APP processing, resulting in enhanced β-amyloid (Aβ) production and formation of amyloid fibrils in vitro. Co-incubation of mutated and wild-type peptides conferred instability on Aβ aggregates and inhibited amyloidogenesis and neurotoxicity. The highly amyloidogenic effect of the A673V mutation in the homozygous state and its anti-amyloidogenic effect in the heterozygous state account for the autosomal recessive pattern of inheritance and have implications for genetic screening and the potential treatment of Alzheimer's disease.

A central pathological feature of Alzheimer's disease (AD) is the accumulation of β-Aβ in the form of oligomers and amyloid fibrils in the brain (*1*). Aβ is generated by sequential cleavage of the APP by β- and γ-secretases and exists as short and long isoforms, Aβ1-40 and Aβ1-42 (*2*). Aβ1-42 is especially prone to misfolding and builds up aggregates that are thought to be the primary neurotoxic species involved in AD pathogenesis (*2*, *3*). AD is usually sporadic, but a small fraction of cases is familial (*4*). The familial forms show an autosomal dominant pattern of inheritance with virtually complete penetrance and are linked to mutations in the APP, presenilin 1, and presenilin 2 genes (*5*). The APP mutations close to the sites of β- or γ-secretase